

Interleaved Continuum-Rigid Manipulation: An Augmented Approach For Robotic Minimally-Invasive Flexible Catheter-based Procedures*

Benjamin L. Conrad, Jinwoo Jung, Ryan S. Penning, and Michael R. Zinn, *Member, IEEE*

Abstract— In recent years, minimally-invasive surgical systems based on flexible robotic manipulators have met with success. One major advantage of the flexible manipulator approach is its superior safety characteristics as compared to rigid manipulators. However, their soft compliant structure, in combination with internal friction, results in poor position and force regulation and has limited their use to simpler surgical procedures. In this paper, we discuss a new approach to continuum robotic manipulation that combines flexible, actively actuated continuum segments with small, limited stroke rigid-link actuators. The small rigid-link joints are interleaved between successive continuum segments and provide a redundant motion and error correction capability. The authors refer to this approach as interleaved continuum-rigid manipulation. In this paper, we describe the overall approach and investigate its performance using a one degree-of-freedom testbed and two degree-of-freedom planar simulation.

Index Terms—catheter, catheter dynamics, control design, flexible manipulator, kinematics, medical robotics, minimally invasive surgery, redundant actuation, tendon drive.

I. INTRODUCTION

While researchers have developed a variety of minimally-invasive surgical (MIS) robotic systems, the majority of MIS manipulation based systems can be classified as either rigid-link manipulators, such as the Intuitive Surgical Da Vinci system [1], or flexible continuum manipulators, such as the Hansen Medical Artisan catheter system [2] or the Stereotaxis Niboe system [3]. One major advantage of the flexible manipulator approach is its superior safety characteristics as compared to rigid manipulators. A compliant structure, in combination with soft atraumatic construction, makes these manipulators much less likely to cause damage when they come in contact with tissue. For these reasons, flexible manipulators, including catheters, have become the dominant interventional tool in applications where safety is of particular concern such as vascular and intracardiac interventional procedures. While MIS systems based on flexible robotic manipulators have met with success, the very features which enable their superior safety characteristics have hindered their use in high performance

manipulation tasks. Their soft compliant structure, in combination with internal friction inherent to their design, results in poor position [4, 5] and force regulation, limiting their use to simpler surgical procedures.

A number of researchers have investigated alternative continuum design approaches, deviating from the tendon-actuated continuum thermoplastic designs found in the vast majority of commercially available flexible medical devices, such as catheters. In general, these approaches have sought to improve performance while maintaining the device's small size and ability to navigate complex paths. In [6-8] a novel concentric tube design is used to achieve a very small device cross-section, facilitating access to small anatomical features. In this case, while device compliance can be kept low, the fundamental trade-off between compliance (for safety) and performance still limits positioning accuracy. In [9-11], a highly articulated, redundant robot probe provides a high degree of maneuverability while maintaining the proximal shape of the probe and thus reducing the chance of injury to sensitive tissue. However, these design approaches employ relatively stiff and/or rigid link construction, potentially compromising the inherent safety embodied by the compliant manipulator concept.

Recently, the use of feedback and associated sensing of flexible MIS robotic manipulators has been explored by a number of investigators to improve the performance of inherently safe flexible continuum manipulators. In [4] a closed-loop system was developed to control end-point position in both task space and joint space. Other examples include [12] where tracking of beating heart motion is explored, [6, 13] where concentric tube manipulators are controlled in position and for end-point stiffness control and [14-19] where various specialized control applications are investigated. Fundamentally, the inherent flexibility and internal friction of flexible medical continuum manipulators, such as cardiac intervention catheters, result in nonlinear hysteresis behavior that limits the closed-loop bandwidth. This, in turn, compromises the devices' ability to reject disturbances at the required time scales. In addition, the nonlinear, non-stationary motion characteristics of these compliant devices often results in limit cycling when used in closed-loop control, reducing the effectiveness of feedback approaches. This is particularly difficult to address for multi-degree-of-freedom manipulators where the hysteresis-induced nonlinear motion is complex and difficult to predict.

*Research supported in part by the Wisconsin Alumni Research Foundation under Grant 101-PRJ61GC. The authors are with the Mechanical Engineering Department, University of Wisconsin-Madison, Madison, WI 53706 USA (email: bconrad@wisc.edu; jjung22@wisc.edu; rpenning@wisc.edu; mzinn@wisc.edu; phone: 608-263-2893; fax: 608-265-2316).

II. AN INTERLEAVED MANIPULATION APPROACH

While the design and feedback approaches previously investigated have provided improvements in the performance of flexible continuum manipulators, none have achieved the performance levels typical of rigid-link designs while maintaining the compliant, atraumatic manipulator characteristics preferred for safety critical applications. The authors believe that the difficulty in achieving both inherent safety and performance is due to fundamental limitations that exist when working with flexible continuum manipulators.

To overcome these challenges we propose a new approach to continuum robotic manipulator design and actuation – where the safety advantages of flexible continuum manipulators is merged with the performance advantages of traditional rigid link manipulators. The approach advocates the combination of flexible, actively actuated continuum segments with small, limited stroke rigid-link actuators. The small rigid-link joints are interleaved between successive continuum segments and provide a redundant motion capability. The authors refer to this approach as *interleaved continuum-rigid manipulation* (see Fig. 1).

The active continuum segments provide large motion capability through, for example, a combination of tendon-driven articulation and telescoping motion. The compliant atraumatic construction of the continuum segments enhance safety while the small size of the rigid-link joints allows both the joint and limited stroke-actuator to be embedded inside the profile of the compliant segments. The limited stroke allows the rigid-link joints to assume a compact form, allowing for the use of a wide variety of micro-scale actuation concepts [20]. The repeatable, predictable motion of the small actuators will allow for active correction of motion errors. The introduction of the small rigid-joints is central to the overall concept – in that they act as *linearizing* elements in a system whose overall behavior is highly nonlinear – thus allowing for effective use of feedback control to enhance performance.

III. KINEMATICS AND CONTROL APPROACH

A. Kinematics

The overall manipulator kinematics description can be developed by considering the kinematics of the flexible

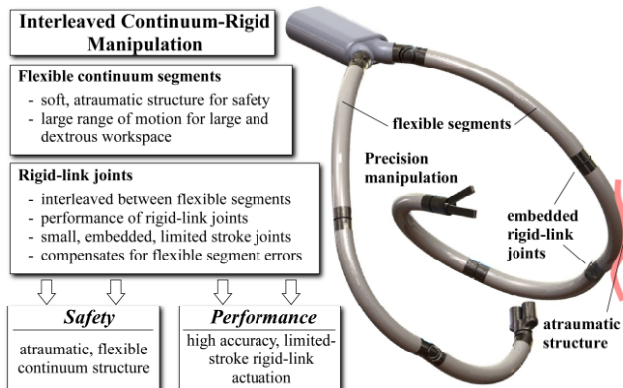


Fig. 1. Conceptual overview of interleaved continuum-rigid manipulation.

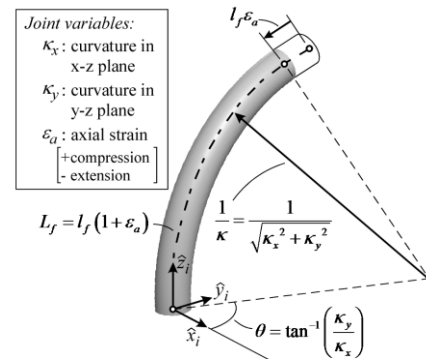


Fig. 2. Kinematic description of the flexible segment.

segment and rigid-link joints separately. The flexible segment kinematics description is a function of the flexible segment actuation and design characteristics. For the purposes of this paper we will limit the discussion to flexible segment articulation only (via application of tension along their control tendons) and exclude motions such as extension (from a proximal segment), or roll (relative to a proximal segment). Additionally, we assume that the flexible segment material behaves linearly in the range of strains to be considered. With these assumptions, we can adopt the kinematic description developed in [14, 21] where the flexible segment motions, or joint variables, are represented by the segment curvatures κ_x and κ_y representing the curvature in the x-z and y-z planes respectively, and the axial strain ϵ_a (see Fig. 2). Assuming a consistent application of control tendon tension, these three joint variables are not independent. For the purposes of this discussion, we assume that the curvatures κ_x and κ_y are independently specified while the axial strain ϵ_a is a dependent variable. This approach assumes that the articulation of the flexible segment results in constant curvature over the complete length of the segment. For this assumption to hold, the effects of internal control tendon friction must be negligible as significant friction would cause the segment curvature to vary as a function of control tendon motion [5].

The kinematics of a single flexible segment can be represented using a homogeneous transformation T_f whose elements are a function of the joint variables (κ_x , κ_y , ϵ_a) (see Appendix A). The rigid link kinematics are a function of the specific joint mechanism design. For the purposes of this discussion, the rigid joint kinematics are represented by homogeneous transformation matrices T_r . The forward kinematics of the complete manipulator are assembled via the chain rule. When the flexible and rigid link degrees-of-freedom are successively alternated, the complete manipulator forward kinematics are given as

$$T = \prod_{i=1}^n (T_r)_i (T_f)_i \quad (1)$$

In this case, the rigid-joint is assumed to be proximal to the corresponding flexible segment. In addition to the forward kinematics, the control approach, discussed in Section III.B, is based on the instantaneous kinematics of the manipulator, which requires the Jacobian relating the flexible segment and rigid-link joint velocities to task space velocities. In this

case, it proves convenient to form the Jacobian numerically using the forward kinematics discussed previously, where the elements of J are the partial derivatives of task motions with respect to joint motions. The task-space Jacobian is represented by J and is partitioned between flexible segment and rigid-link motions

$$J = [J_f | J_r]. \quad (2)$$

B. Control and Localization Approach

One of the central challenges of the interleaved approach is formulating an effective control strategy. There have been many formal methods developed for multi-input-multi-output control system design including μ -synthesis, H_∞ , and, more recently, design approaches developed for dual-input-single-output system, such as the PQ approach [22]. These approaches are worth consideration, however in this application the rigid link and flexible segment are not completely redundant actuators. While the manipulability of these two actuators must overlap, we expect that the rigid link will generally be of greater precision, have less actuation range, and possibly be faster than the flexible segment actuator. These actuator differences, in addition to the nonlinear properties of the catheter, suggest a parallel control structure where the flexible segment controller acts on the error between the task space motion command x_d and the measured motion of the flexible segment x_f^* (see Fig. 3). This approach is motivated by the desire to limit the motion of the limited-stroke rigid-link joints while correcting for motion errors that result from flexible segments. The flexible segment task motion x_f^* is formed by subtracting the motion attributable to the rigid-link joint motion x_r^* from the measured total device motion x^* .

The flexible segment control includes a feed-forward inverse kinematics block which converts the desired task space configuration to flexible segment joint commands (i.e. segment curvatures). For the two degree-of-freedom system discussed in section IV.A as well as the one degree of freedom experimental testbed discussed in section IV.B, the inverse kinematics pertaining to the coupled motion of the flexible sections (exclusive of rigid link joint motion) are obtained using a multivariable Newton's method. The Jacobian J_f relating flexible segment joint velocities to the

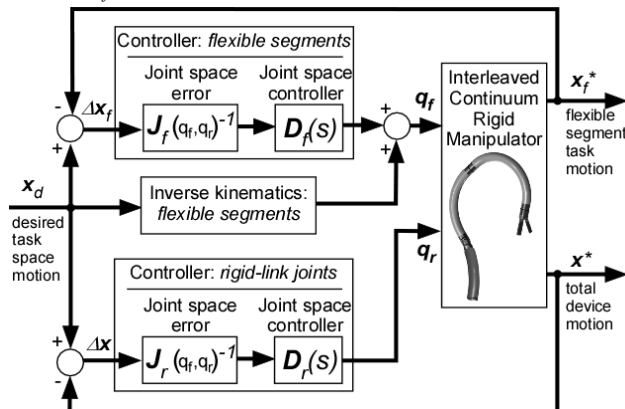


Fig. 3. Overview of a candidate interleaved continuum rigid manipulator control structure.

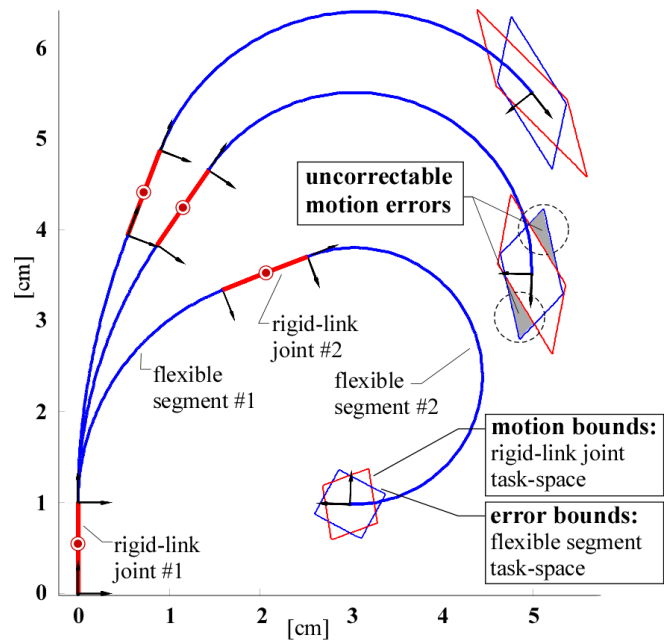


Fig. 4. Task-space error and motion bounds of the flexible segment and rigid-link joints. The proximal and distal flexible segment articulation errors depicted are ± 0.10 radian and ± 0.15 radian, respectively. The rigid-link joint range of motion depicted is ± 0.10 radian.

task-space velocities is used in the iterative solver. The controller, which acts on the error associated with the flexible segment alone, transforms the task space error to equivalent joint space (of the flexible segments) via the flexible segment Jacobian J_f . The joint space error is fed through a compensation block $D_f(s)$ whose output is summed with the feed-forward term to produce the flexible segment joint space position command q_f . The rigid-link joint controller acts on the error defined as the difference between the desired task space motion command x_d and the total measured device motion x^* . This error is transformed from task space to the rigid-link joint space via the rigid-link joint Jacobian J_r . This joint space error is then fed through a compensation block $D_r(s)$ to produce the rigid-link joint space position command q_r .

It should also be noted that both the flexible segment Jacobian J_f and rigid-link joint Jacobian J_r are functions of the manipulator's configuration. As a result, knowledge of the configuration is required—either through estimation or direct measurement. While the rigid-link joint positions are likely to closely track the desired rigid-link motions, the flexible segments are expected to have significant error and thus direct measurement of their motion is required to properly form the Jacobian for both the flexible segments and rigid-link joints.

Finally, the kinematic design will have a significant effect on the performance of the manipulator. As described earlier, the primary function of the limited-stroke rigid link joints is to compensate for flexible segments motion errors. As such, the task space motion bounds of the rigid-link joints should envelope the task-space error bounds of the flexible segments. An example two degree of freedom manipulator,

overlaid with the error and motion bounds of the flexible and rigid-link joints respectively, is shown in Fig. 4. The regions of uncorrectable error are a function of the rigid-link joints range of motion, the error range of the flexible segments, and the configuration of the manipulator.

IV. EVALUATION

The interleaved continuum rigid manipulator approach was evaluated experimentally, using a one degree of freedom validation testbed, and evaluated via simulation, using a two degree of freedom planar manipulator simulation. The results of this evaluation are presented in the following sections.

A. Simulation Investigation

A two degree-of-freedom planar manipulator simulation was developed to explore the effects of dynamic coupling and internal friction in the flexible segment. This platform also enables development of control approaches for multiple degree of freedom manipulators.

The flexible segments are modeled by a serial chain of links constrained by revolute joints (see Fig. 5). Flexible segment bending compliance and internal damping were modeled with parallel springs and dampers which act across the revolute joint. Flexible segment control inputs, applied via control tendon tension, are applied as torques at the revolute joints where the tension magnitude and local curvature determine the magnitude of the applied torques. To model the effects of internal control tendon friction, which can have a significant effect on flexible segment motion, a modified Dahl friction model was used – where the steady-state Dahl friction torque is related to control tendon tension as well as local flexible segment curvature [5]. For simplicity, the modified Dahl friction torques were applied directly at the joints, as opposed to [5] which applied forces at the tendon sliding interface.

The rigid-link joints are modeled as revolute joints which can impose a displacement between successive flexible segments. The implicit assumption being that the rigid link joints have output impedance that is sufficiently high such that the dynamics of the flexible segments have negligible effect on their relative position. In addition, the simulation assumes that the rigid links are designed such that the flexible segment control tendon tension and rigid-link joint motion are uncoupled. This uncoupling can be achieved by routing the control tendons across the rigid-link joints such that joint motion does not result in a control tendon length change (thus resulting in no work being done - see Fig. 8 in Section IV.B).

The control structure implemented in the simulation was described in section III.B. Task space motion is defined as the planar position of the tip of the manipulator. In this case, the flexible and rigid link compensations, $D_f(s)$ and $D_r(s)$, consisted of simple integral controllers. The choice of an integral controller is motivated by the open-loop uncompensated system dynamics. At frequencies below the first flexible mode of the manipulator, the task space motion,

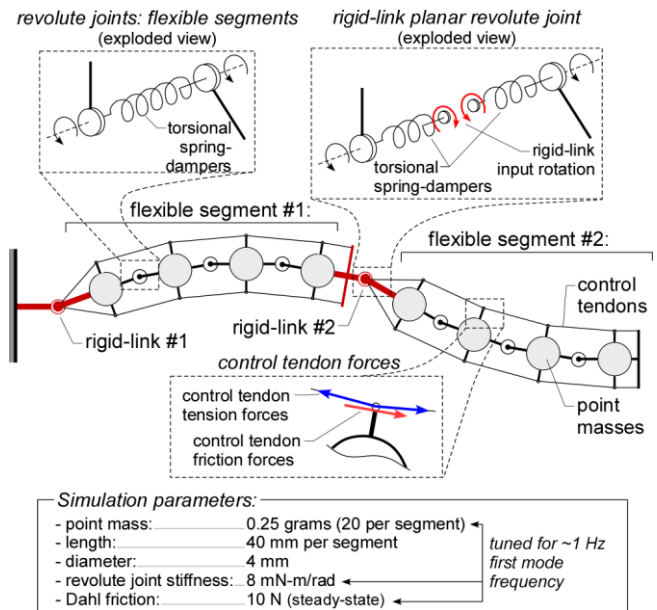


Fig. 5. Overview of two degree-of-freedom planar simulation model.

in this case planar tip translation, is related to the input joint motions (e.g. flexible segment curvature and rigid link rotations) by a simple gain, with no phase distortion. The integral controller was chosen to achieve a cross-over frequency below the first mode frequency, while maintaining sufficient gain margin. Use of alternative compensation approaches are limited by the manipulator's flexible modes. For example, use of simple proportional control action would place the cross-over frequency above the frequency of the first flexible mode, likely resulting in instability.

The planar simulation described above was used to evaluate the performance of the interleaved continuum-rigid manipulation approach and compare it to flexible segment manipulator control. The flexible segment manipulator was controlled using the same control structure as the interleaved system, absent the rigid link motion and control. The controller gains were adjusted upward until signs of instability were observed. As a baseline, both approaches were compared to a flexible segment manipulator without feedback control. In the first simulation experiment, the manipulator was positioned approximately in the center of its workspace. A small motion (5 mm) step input command was applied and the position control performance was simulated. The results of the simulation are shown in Fig. 6. As seen in Fig. 6, the uncompensated flexible segment manipulator response shows a time constant of approximately 0.5 seconds with a steady-state error of 0.6 mm. In this case, the steady-state error is a result of the internal control tendon friction. In the case of the flexible segment manipulator with closed-loop control, the response shows improvement as compared to the uncompensated flexible segment manipulator, specifically in regards to the elimination of the steady-state error. However, due to the limitations in the flexible segment controller, the response time is significantly increased from the uncontrolled state. Finally, the response of the interleaved manipulator under closed-loop control shows significant improvement as

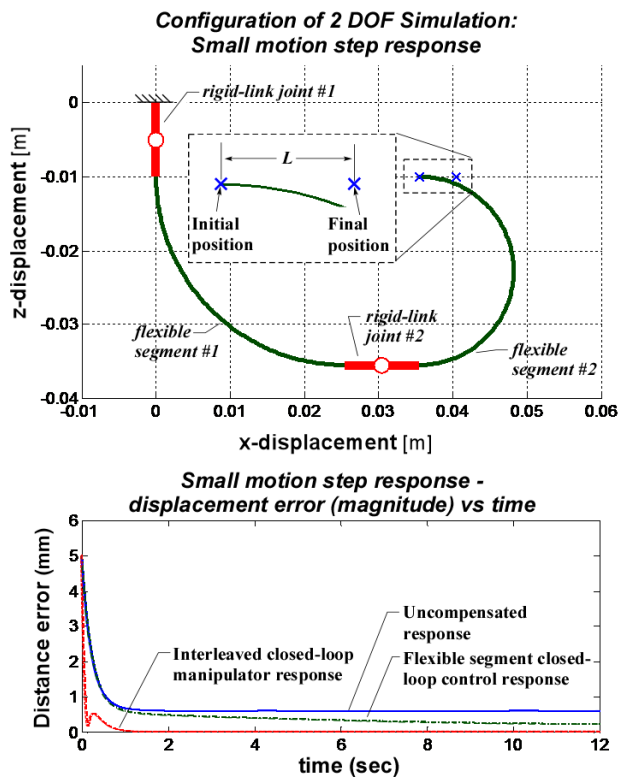


Fig. 6. Small motion step input simulation results. The spike in the interleaved response results from the catheter dynamics being slower than the rigid link actuator.

compared to the flexible segment manipulator. Both the speed of the initial response, as well as the speed in which the error is driven to zero, have improved. In this case, the time constant of the interleaved system is approximately one third that of the closed-loop flexible segment manipulator.

In the second simulation experiment, the manipulator was commanded along a circular trajectory of 20 mm radius. The tracking time to complete one revolution was 32 seconds. The trajectory tracking results in Fig. 7 show the motion of the tip of the manipulator after three complete cycles, to allow hysteresis effects to reach steady state. As seen in Fig. 7, the uncompensated flexible segment manipulator exhibits significant tracking error, as the effects of internal control tendon friction distort the deflection of the flexible segments. In the case of the flexible segment manipulator with closed-loop control, the tracking response shows improvement as compared to the uncompensated flexible segment manipulator. However, the tracking errors are still significant as the speed of the controller is not high enough to compensate for the change in friction due to the moving internal control tendons. Finally, the tracking response of the interleaved manipulator under closed-loop control shows almost an order of magnitude reduction in position error as compared to the flexible segment manipulator.

B. Experimental Validation

A one degree-of-freedom testbed was developed to further investigate the potential of interleaved catheter actuation.

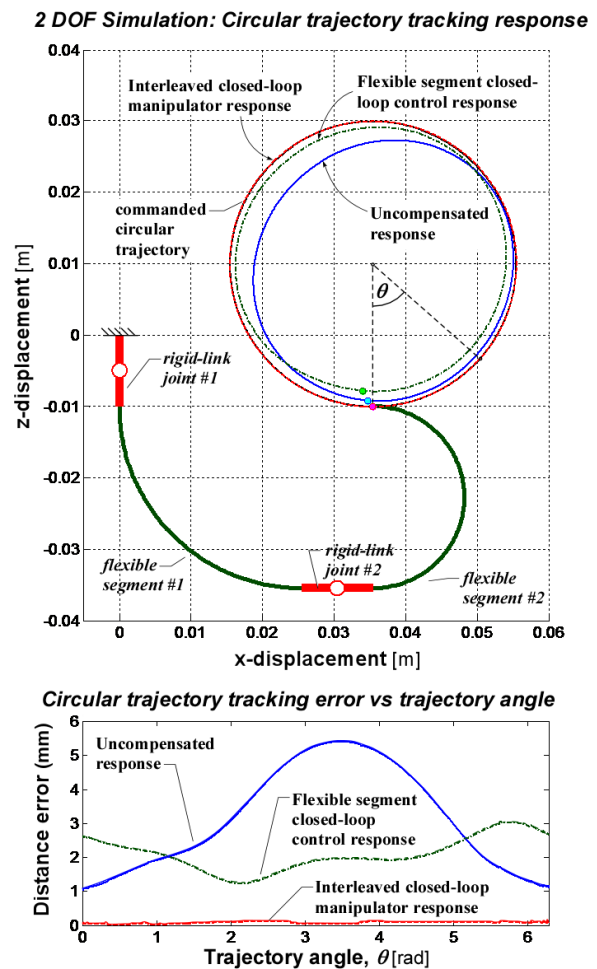


Fig. 7. Trajectory tracking simulation results. Note that the excellent interleaved response enjoys nearly ideal compensation of control tendon friction, beyond that attainable in a real system.

The major components of the testbed are shown in Fig. 8. The testbed was designed to actuate a flexible catheter prototype in articulation (i.e. bending). The articulation of the flexible segment is accomplished through actuation of opposing control tendons. The control tendons are routed close to the surface of the catheter through guide lumens and are fixed at the distal end of the catheter. Actuation of the tendons causes the catheter to articulate within a vertical plane. The amount of articulation is related to control tendon motion through the kinematics discussed in Section III.A. For the testbed rigid link actuator T_r is found by considering the slider-crank mechanism visible in Fig. 8.

The rigid-link joint motion provides rotation about a pivot axis located at the base of the flexible segment. The flexible segment control tendons intersect the rotation axis of the rigid-link to eliminate coupling between the flexible and rigid-link motions. The rigid-link joint rotation is actuated via a voice-coil actuator through a slider-crank mechanism. As mentioned above, our present focus is on investigating the advantages of interleaved actuation. The testbed is not intended as a design prototype and, as such, we have made no attempt at rigid-link miniaturization.

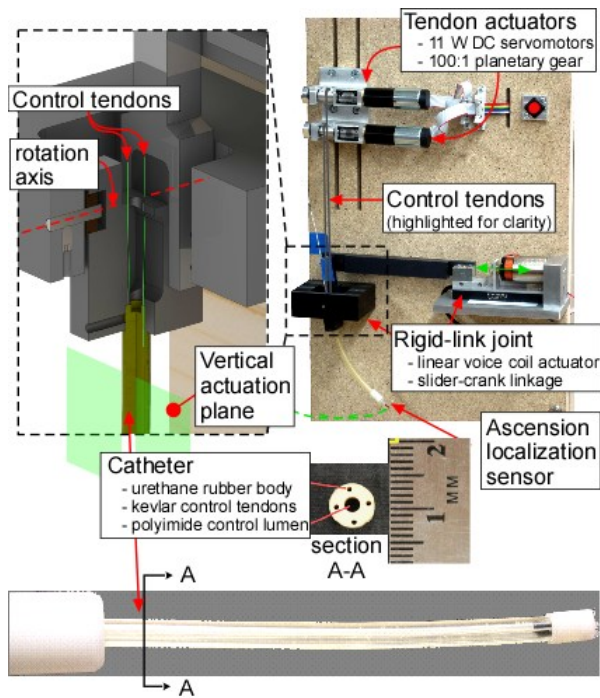


Fig. 8. Overview of one degree-of-freedom interleaved continuum-rigid manipulation testbed.

The control structure implemented on the prototype is identical to the one described in section III.B. Task space motion is defined as the horizontal position of the tip of the catheter. As above, the flexible and rigid link compensation, $D_f(s)$ and $D_r(s)$, consisted of simple integral controllers. The choice of an integral controller is motivated by the open-loop uncompensated system dynamics (see Section IV.A). Catheter tip motion is acquired with an Ascension trakStar 3D magnetic position sensor, operating at 200 Hz, providing a globally-referenced measurement of the catheter's tip position. The controller and sensor input is implemented using Matlab xPC 2009a.

The testbed described above was used to evaluate the performance of the interleaved continuum-rigid manipulation approach and compare it to flexible segment manipulator control. The flexible segment manipulator was controlled using the same control structure as the interleaved system, absent the rigid link motion and control. As a baseline, both approaches were compared to a flexible segment manipulator without feedback control. In the experiment, the manipulator was positioned approximately in the center of its workspace (vertical). A sequence of step impulses was commanded and the position control performance was measured. The results of the experiments are shown in Fig. 9.

The uncompensated flexible segment manipulator ('Open Loop' in Fig. 9) response shows a steady-state error of 50%. In this case, the steady-state error is a result of errors in the open loop device kinematics as well as control tendon friction. In the case of the flexible segment manipulator with closed-loop control, the response shows improvement as compared to the uncompensated flexible segment manipulator, specifically in regards to the elimination of the

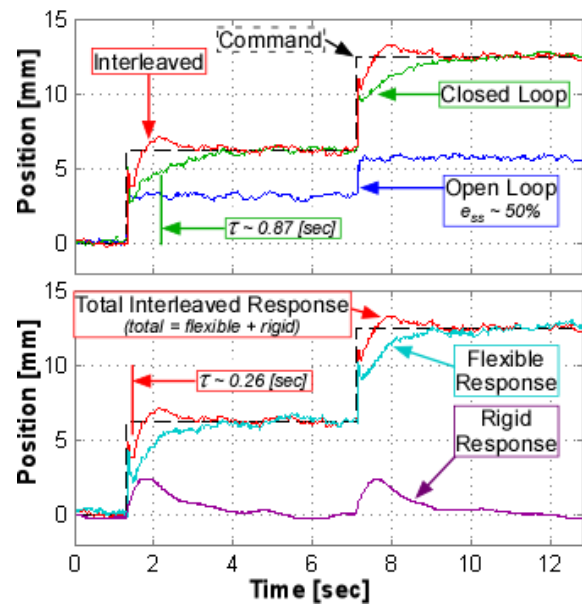


Fig. 9. Top: position responses to successive step impulse commands for the discussed controllers. Bottom: contributions to the interleaved response from the flexible segment and rigid link.

steady-state error. The response time is significantly increased from the uncontrolled state, with a time constant of 0.87 seconds. Finally, the response of the interleaved manipulator under closed-loop control shows improvement as compared to the flexible segment manipulator. Both the speed of the initial response as well as the speed in which the error is driven to zero has improved. In this case, the time constant of the interleaved system is approximately three times that of the closed-loop flexible segment manipulator. The lower pane of Fig. 9 dissects the interleaved controller response. The catheter tip position is the linear combination of the flexible segment and rigid link motions. Interpreting the controller topology given in Fig. 3, receipt of a step command immediately commands a large motion to the flexible segment (the immediate spike in the aqua 'Flexible Response') while the integral gains in D_f and D_r begin accumulating the position error into their respective actuator commands. The closed loop position bandwidth of both the rigid link and flexible segment actuators are limited by the catheter's first vibrational mode (~ 5 Hz). However the nonlinear interaction of the compliant flexible structure and control tendons further limits the flexible segment bandwidth to 1.1 Hz, compared to 3.8 Hz for the rigid link actuator. Fig. 9 also demonstrates that the interleaved control topology naturally returns the rigid link (the purple, 'Rigid Response') to its home position as the flexible segment achieves its command. This maximizes control bandwidth for subsequent commands, limited only by catheter dynamics.

V. DISCUSSION

As discussed earlier, the advantages of the interleaved approach lie in its ability to compensate for flexible segment motion errors when these errors cannot be addressed through closed-loop flexible segment control alone. While use of

feedback for robotic catheter control has been successful [4, 6, 12-19], in situations where significant nonlinear, non-stationary behavior is observed, closed-loop control can break down [5]. In general, this phenomenon is observed in multi-degree of freedom catheter devices, such as the Hansen Medical Artisan catheter [2]. In this case, the combination of bi-planar catheter articulation and telescoping motion (from a supporting sheath) result in significant frictional forces, both between the control tendons and control lumens and between the telescoping segments. The frictional forces and compliant catheter structure interact to create significant hysteresis. This behavior has been observed both anecdotally (by the communicating author) and investigated more formally in [5]. Similarly, this behavior is reflected in the results presented here, where the performance improvements of the two degree simulation were significantly greater than those displayed in the one degree-of-freedom testbed. In this case, the effect of device friction was not large enough to significantly alter the instantaneous kinematics of the system. Thus, the performance of the flexible closed loop system was as effective, if albeit slower than, the interleaved system.

APPENDIX

A. Flexible Segment Kinematics

The kinematics of a single flexible segment can be represented using a homogeneous transformation T_f .

$$T_f = \begin{bmatrix} R_f & \vec{P}_f \\ 0 & 1 \end{bmatrix}. \quad (A1)$$

The rotation matrix R_f can be evaluated using the axis-angle representation [23] for a rotation α about a fixed axis \hat{k} .

$$R_f = \begin{bmatrix} k_x^2 v_\alpha + c_\alpha & k_x k_y v_\alpha - k_z s_\alpha & k_x k_z v_\alpha + k_y s_\alpha \\ k_x k_y v_\alpha + k_z s_\alpha & k_y^2 v_\alpha + c_\alpha & k_y k_z v_\alpha - k_x s_\alpha \\ k_x k_z v_\alpha - k_y s_\alpha & k_y k_z v_\alpha + k_x s_\alpha & k_z^2 v_\alpha + c_\alpha \end{bmatrix}. \quad (A2)$$

where

$$c_\alpha = \cos \alpha, s_\alpha = \sin \alpha, v_\alpha = 1 - \cos \alpha. \quad (A3)$$

The rotation magnitude α is given as

$$\alpha = \kappa L_f. \quad (A4)$$

where the length of the flexible segment L_f and the total curvature κ are given as

$$L_f = l_f(1 + \varepsilon_\alpha) \quad (A5)$$

$$\kappa = \sqrt{\kappa_x^2 + \kappa_y^2}. \quad (A6)$$

l_f is the undeformed length of the flexible segment. The unit vector about which the rotation occurs is given as

$$\hat{k} = [k_x \ k_y \ k_z]^T = [-\sin \theta \ \cos \theta \ 0]^T \quad (A7)$$

where roll angle θ is evaluated by

$$\theta = \tan^{-1}(\kappa_y / \kappa_x). \quad (A8)$$

The position vector \vec{P}_f is given as

$$\vec{P}_f = \begin{bmatrix} x_f \\ y_f \\ z_f \end{bmatrix} = \frac{1}{\kappa} \begin{bmatrix} (1 - \cos \alpha) \cos \theta \\ (1 - \cos \alpha) \sin \theta \\ \sin \alpha \end{bmatrix}. \quad (A9)$$

REFERENCES

- [1] *Intuitive Surgical, Inc.* Available: <http://www.intuitivesurgical.com>
- [2] *Hansen Medical, Inc.* Available: <http://www.hansenmedical.com/>
- [3] Stereotaxis. *NIOBE® Magnetic Navigation System.* Available: www.stereotaxis.com
- [4] R. S. Penning, J. Jung, J. A. Borgstadt, N. J. Ferrier, and M. R. Zinn, "Towards closed loop control of a continuum robotic manipulator for medical applications," in *Robotics and Automation (ICRA), IEEE International Conference on*, 2011, pp. 4822-4827.
- [5] J. Jung, R. S. Penning, N. J. Ferrier, and M. R. Zinn, "A Modeling Approach for Continuum Robotic Manipulators: Effects of Nonlinear Internal Device Friction," presented at the 2011 IEEE/RSJ International Conference on Intelligent Robots and Systems (IROS), San Francisco, 2011.
- [6] P. E. Dupont, J. Lock, B. Itkowitz, and E. Butler, "Design and Control of Concentric-Tube Robots," *Robotics, IEEE Transactions on*, vol. 26, pp. 209-225, 2013.
- [7] R. Webster, J. Swensen, J. Romano, and N. Cowan, "Closed-Form Differential Kinematics for Concentric-Tube Continuum Robots with Application to Visual Servoing," in *Experimental Robotics*, vol. 54, O. Khatib, V. Kumar, and G. Pappas, Eds., ed: Springer Berlin / Heidelberg, 2009, pp. 485-494.
- [8] R. J. Webster, J. M. Romano, and N. J. Cowan, "Mechanics of Precurved-Tube Continuum Robots," *Robotics, IEEE Transactions on*, vol. 25, pp. 67-78, 2009.
- [9] H. Choset and W. Henning, "A follow-the-leader approach to serpentine robot motion planning," *ASCE Journal of Aerospace Engineering*, vol. 12, pp. 65-73, 1999.
- [10] A. Degani, H. Choset, A. Wolf, T. Ota, and M. A. Zenati, "Percutaneous Intrapericardial Interventions Using a Highly Articulated Robotic Probe," in *Biomedical Robotics and Biomechanics (BioRob), The First IEEE/RAS-EMBS International Conference on*, 2006, pp. 7-12.
- [11] A. Degani, H. Choset, A. Wolf, and M. A. Zenati, "Highly articulated robotic probe for minimally invasive surgery," in *Robotics and Automation (ICRA), Proceedings IEEE International Conference on*, 2006, pp. 4167-4172.
- [12] S. G. Yuen, D. T. Kettler, P. M. Novotny, R. D. Plowes, and R. D. Howe, "Robotic Motion Compensation for Beating Heart Intracardiac Surgery," *The International Journal of Robotics Research*, pp. 1355-1372, 2009.
- [13] M. Mahvash and P. E. Dupont, "Stiffness Control of Surgical Continuum Manipulators," *Robotics, IEEE Transactions on*, vol. 27, pp. 334-345, 2011.
- [14] D. B. Camarillo, C. R. Carlson, and J. K. Salisbury, "Configuration tracking for continuum manipulators with coupled tendon drive," *IEEE Transactions on Robotics*, vol. 25, pp. 798-808, 2009.
- [15] X. Kai and N. Simaan, "An Investigation of the Intrinsic Force Sensing Capabilities of Continuum Robots," *Robotics, IEEE Transactions on*, vol. 24, pp. 576-587, 2008.
- [16] F. Arai, M. Ito, T. Fukuda, M. Negoro, and T. Naito, "Intelligent assistance in operation of active catheter for minimum invasive surgery," in *RO-MAN '94 Nagoya, Proceedings., 3rd IEEE International Workshop on Robot and Human Communication*, 1994, pp. 192-197.
- [17] Y. Bailly, A. Chauvin, and Y. Amirat, "Control of a high dexterity micro-robot based catheter for aortic aneurysm treatment," in *Robotics, Automation and Mechatronics, 2004 IEEE Conference on*, 2004, pp. 65-70.
- [18] V. K. Chitrakaran, A. Behal, D. M. Dawson, and I. D. Walker, "Setpoint regulation of continuum robots using a fixed camera," *Robotica*, vol. 25, pp. 581-586, 2007.
- [19] X. Kai and N. Simaan, "Actuation compensation for flexible surgical snake-like robots with redundant remote actuation," in *Robotics and Automation (ICRA), Proceedings IEEE International Conference on*, 2006, pp. 4148-4154.
- [20] N. T. Inc. *SQUIGGLE micro piezoelectric motor technology.* Available: <http://www.newscaletech.com/>
- [21] D. B. Camarillo, C. F. Milne, C. R. Carlson, M. R. Zinn, and J. K. Salisbury, "Mechanics Modeling of Tendon-Driven Continuum Manipulators," *Robotics, IEEE Transactions on*, vol. 24, pp. 1262-1273, 2008.
- [22] S. J. Schroeck, W. C. Messner, and R. J. McNab, "On compensator design for linear time-invariant dual-input single-output systems," *Mechatronics, IEEE/ASME Transactions on*, vol. 6, pp. 50-57, 2001.
- [23] M. W. Spong, S. Hutchinson, and M. Vidyasagar, *Robot modeling and control.* John Wiley & Sons Hoboken, NJ, 2006.